

Representing Videos as Discriminative Sub-graphs for Action Recognition*

Dong Li[†], Zhaofan Qiu[‡], Yingwei Pan[‡], Ting Yao[‡], Houqiang Li[†], and Tao Mei[‡]

[†] University of Science and Technology of China, Hefei, China [‡] JD AI Research, Beijing, China

{dongli1995.ustc, zhaofanqiu, panyw.ustc, tingyao.ustc}@gmail.com

lihq@ustc.edu.cn, tmei@jd.com

Abstract

Human actions are typically of combinatorial structures or patterns, i.e., subjects, objects, plus spatio-temporal interactions in between. Discovering such structures is therefore a rewarding way to reason about the dynamics of interactions and recognize the actions. In this paper, we introduce a new design of sub-graphs to represent and encode the discriminative patterns of each action in the videos. Specifically, we present Multi-scale Sub-graph LEarning (MUSLE) framework that novelly builds space-time graphs and clusters the graphs into compact sub-graphs on each scale with respect to the number of nodes. Technically, MUSLE produces 3D bounding boxes, i.e., tubelets, in each video clip, as graph nodes and takes dense connectivity as graph edges between tubelets. For each action category, we execute online clustering to decompose the graph into sub-graphs on each scale through learning Gaussian Mixture Layer and select the discriminative sub-graphs as action prototypes for recognition. Extensive experiments are conducted on both Something-Something V1 & V2 and Kinetics-400 datasets, and superior results are reported when comparing to state-of-the-art methods. More remarkably, our MUSLE achieves to-date the best reported accuracy of 65.0% on Something-Something V2 validation set.

1. Introduction

The recognition of human actions is to analyze a video and identify the actions taking place in the video. In general, an action arises from interactive motion, and involves actors, objects and functional interactions in between. This characteristics motivate us to represent the structure of a video as a spatio-temporal graph. The graph nodes correspond to the volumes of actor or object regions in space-time and the edges capture the interactions between the volumes. Then, a valid question is how to reason about such



(a) Skateboarding



(b) Assembling computer

Figure 1. Two example videos of the action of “skateboarding” and “assembling computer,” respectively.

graph structure to recognize the action. The difficulty originates from two aspects: 1) is it necessary to capitalize on the whole graph for reasoning? 2) considering the fact that the complexity of different actions is various, how to discover and model the discriminative patterns for each action in a unified framework?

In an effort to answer the two questions, let’s look at the two action instances illustrated in Figure 1. In the upper video clip of action “skateboarding,” the objects contain “building,” “pole,” “plants,” and “skateboard.” Nevertheless, the action of “skateboarding” only involves the actor (person), the object of “skateboard,” and the occurring interactions. In other words, the action is irrelevant to the other objects and only necessitates using a part of video structure (graph). As a result, we propose to mitigate this issue through learning discriminative sub-graphs as the prototypes of each action category rather than performing reasoning on the whole graph. The design of such prototypes takes the advantages of clustering on sub-graphs, on one hand, offers greater discriminative power in recognition, and on the other, is helpful for encoding intra-class variance. Compared to the upper video in which the action is related to only one object “skateboard,” the lower one of action “assembling computer” correlates with more objects, including “screwdriver,” “computer parts,” and “computer.” From this view, the action “assembling computer” is relatively more complex and thus its prototypical sub-graphs should include more nodes. To take the complexity of actions into account, the framework should enable flexibility in the scale of sub-graphs, i.e., the number of nodes in sub-graphs, to better reflect the inherent properties of different actions.

*This work was performed at JD AI Research.

To consolidate the idea of modeling discriminative sub-graphs in videos for various actions, we present Multi-scale Sub-graph LEarning (MUSLE) framework for action recognition. Specifically, we evenly divide an input video into a set of fixed-length video clips, which are fed into Tubelet Proposal Networks (TPN) to produce space-time actor/object tubelets. Technically, we leverage Faster R-CNN pre-trained on COCO dataset to initialize the region proposals in the first frame, and then estimate the movement of each proposal frame by frame in each clip to finally link the volume of proposals across frames as tubelets. The representation of each tubelet is the concatenation of visual features plus the coordinates of its constituent proposals. Our MUSLE takes all the tubelets from clips in a video as graph nodes and exploits dense connectivity as graph edges, which measure both semantic similarity and relative coordinate changes between every two nodes. Next, MUSLE decomposes the whole graph into multiple scales of sub-graphs. Each scale corresponds to a fixed number of nodes in the sub-graphs. We capitalize on one Gaussian Mixture Layer to interpret the distribution of all the sub-graphs from an identical action on each scale and learn K Gaussian kernels. Each kernel is regarded as the discriminative sub-graph or action prototype on that scale. Note that we optimize our MUSLE framework in an end-to-end manner. During inference, we compute the similarity between sub-graphs extracted from the test video and action prototypes across all the scales and actions, and take the class of action prototype with the highest similarity as prediction.

The main contribution of this work is the proposal of representing video structure as a space-time graph and eventually discovering the discriminative sub-graphs for action recognition. This also leads to the elegant views of how to perform end-to-end learning of the discriminative sub-graphs, and how to nicely present the complexity of different actions in the reasoning process, which are problems not yet fully understood. We demonstrate the effectiveness of our design, i.e., MUSLE framework, on Something-Something V1&V2 and Kinetics-400 datasets, and superior performances are reported in the experiments.

2. Related Works

Action Recognition is a fundamental computer vision task and has been extensively studied recently. Early approaches usually rely on hand-crafted features, which detect spatio-temporal interest points and then describe these points with local representations [45, 46]. With the tremendous success of deep convolution networks on image-based classification tasks [12, 35, 38, 41], researchers started to explore the application of deep networks on video action recognition task [7, 18, 29, 30, 54]. In [37], the famous two-stream architecture is devised by applying two 2D CNN architectures separately on visual frames and staked opti-

cal flows. This two-stream architecture is further extended by exploiting sparse temporal sampling [47], convolutional fusion [9], convolutional encoding [6, 31], and spatio-temporal attention [20]. [55] highlights a drawback of two-stream architecture that exploits a standard image CNN instead of a specialized network for training videos, which makes the two-stream network unable to capture long-term temporal information. To address this issue, Tran *et al.* [42] propose a 3D CNN (i.e., C3D) for learning video representation, which performs 3D convolutions on adjacent frames to jointly model the spatial and temporal features. Compared to 2D CNN, C3D holds much more parameters and is difficult to obtain good convergence. Consequently, I3D [2] further takes advantage of ImageNet pretraining by inflating 2D CNN into 3D. To reduce the heavy computations of 3D CNNs, several methods are proposed to find the trade-off between precision and speed [27, 32, 43, 50, 59]. For example, P3D [32] and R(2+1)D [43] decompose the 3D convolution into a 2D spatial convolution and a 1D temporal convolution. TSM [27] shifts the features across the channel dimension to perform temporal modeling. LGD [33] further devises a two-pathway architecture to learn local and global representations in parallel. In this work, we imitate the design of LGD in the backbone of tubelet feature extractor, but our measure of interactions among actors or objects could be readily integrated into any advanced networks.

Graphical Models have been proven to be helpful for relation reasoning in various computer vision tasks, such as semantic segmentation [1, 3, 26] and image captioning [52, 53, 57]. Neural networks that operate on graphs have previously been introduced as a form of RNN in early works [5, 25, 36]. Thanks to the proposal of Graph Convolutional Networks (GCN) [16] which generalize the convolutional operation to deal with graph-structured data, many graph-based methods have been devised for action recognition in recent years, especially for skeleton-based action recognition. For example, ST-GCN [51] proposes a spatio-temporal graph to model the structured information among the human joints. Different from skeleton-based action recognition where the skeleton data can be naturally seen as graph structure, generic action recognition methods employ GCNs to model the relations between fixed regions or objects. For example, [4, 23, 44] adopts GCN to build a reasoning module to model the relations between disjoint and distant regions. [21, 48] takes dense object proposals as graph nodes and learns the relations between them. [22] treats each object proposal detected in the sample frames as a graph node and then searches adaptive network structures to model the object interactions. Unlike aforementioned graphical techniques for action recognition which perform relation reasoning over the complete graph, our work contributes by discovering the discriminative sub-graphs across different scales for facilitating spatio-temporal reasoning.

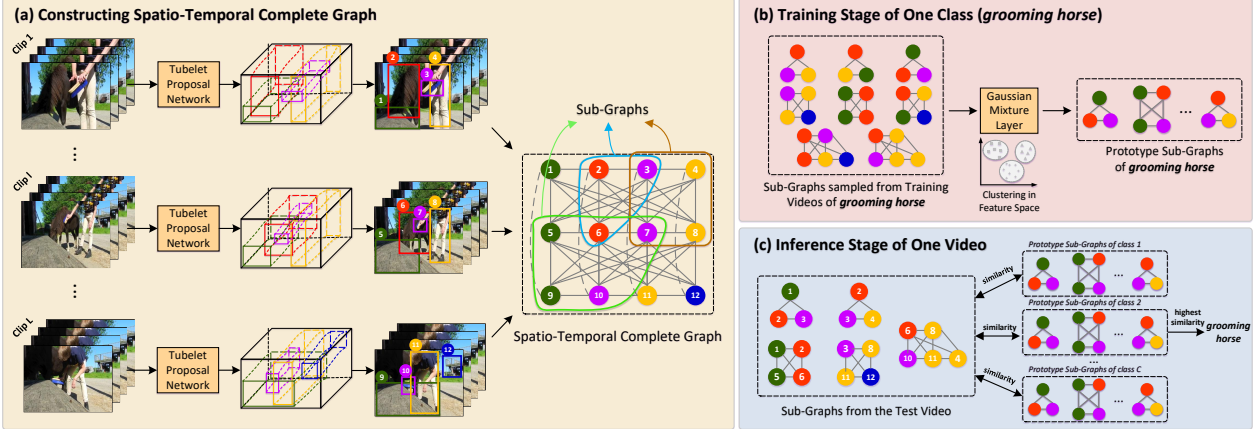


Figure 2. An overview of our MUSLE framework. (a) Given an input video, L video clips are produced by evenly dividing this video. All clips are fed into Tubelet Proposal Networks to produce space-time actor/object tubelets in parallel. Next, by taking all tubelets as graph nodes and exploiting dense connectivity as edges, we build a spatio-temporal complete graph to perform reasoning. After that, MUSLE decomposes the whole graph into sub-graphs with multiple scales. (b) During training, conditioned on all the sub-graphs from an identical action on each scale, a Gaussian Mixture Layer is learnt to discover the discriminative sub-graphs or action prototypes for that action. (c) At inference, after extracting all sub-graphs across different scales from the test video, we calculate the similarity between all sub-graphs and action prototypes across all the scales and actions. The class of action prototype with the highest similarity is thus taken as the prediction.

3. Multi-scale Sub-graph Learning

In this paper, we devise a Multi-scale Sub-graph LEarning (MUSLE) framework to exploit the discriminative sub-graphs across different scales for facilitating spatio-temporal reasoning. Figure 2 depicts an overview of our architecture for action recognition. The training process of MUSLE consists of three main components: tubelet generation, spatio-temporal complete graph construction, and discriminative sub-graph extraction. Specifically, given the set of video clips evenly divided from the input video, we leverage Tubelet Proposal Networks (TPN) to generate space-time actor/object tubelets for each video clip. After that, a spatio-temporal complete graph is constructed by taking all the tubelets within a video as graph nodes and exploiting dense connectivity as edges. We further decompose such complete graph into a series of sub-graphs across different scales. For each scale, a Gaussian Mixture Layer is learnt to extract the discriminative sub-graphs or action prototypes. During inference, we extract sub-graphs from each test video, and further measure the similarity between the extracted sub-graphs and action prototypes across all the scales and actions. The action category of action prototype with the highest similarity is finally taken as the prediction.

3.1. Tubelet Proposal Networks

The Tubelet Proposal Networks (TPN) targets for producing the actor/object tubelets, i.e., the volume of actor/object proposals across consecutive frames, within each video clip. Here we remould TPN in [19] by migrating it from actor-only tubelet generation to our scenario of both actor and object tubelet generation. Concretely, we first capitalize on an actor/object detector to find actor/object

proposals in the start frame of each clip. The TPN further estimates the movements of each proposal in current frame to produce the corresponding proposal in the subsequent frame. The volume of proposals across consecutive frames are finally linked as the tubelets within that clip.

Formally, given a video clip with T frames, we firstly adopt Faster R-CNN pre-trained on COCO dataset [28] to detect the actor/object region proposals in the first frame. We keep the top- M proposals $B_1 = \{b_1^m | m = 1, \dots, M\}$ with the highest detection scores as the proposal set of the first frame. Next, conditioned on the t -th frame I_t and its proposal set B_t , TPN produces the proposal set B_{t+1} for the next frame I_{t+1} recurrently. Specifically, for each proposal b_t^m in t -th frame I_t , we estimate the movement of b_t^m in the next frame I_{t+1} depending on the visual features of the same location of b_t^m across the two frames. Here we directly define the outputs of ROI pooling in I_t and I_{t+1} for the same location of b_t^m as the visual features \mathbf{F}_t^m and $\mathbf{F}_{t+1}^m \in \mathbb{R}^{w \times h \times d}$, where w , h and d are width, height and channel numbers. A bilinear kernel is further utilized to capture the pairwise correlations and model spatial interactions between \mathbf{F}_t^m and \mathbf{F}_{t+1}^m for movement estimation:

$$\begin{aligned} \langle \mathbf{F}_t^m, \mathbf{F}_{t+1}^m \rangle_2 &= \frac{1}{S^2} \sum_{i=1}^S \sum_{j=1}^S \langle \mathbf{F}_{t,i}^m, \mathbf{F}_{t+1,j}^m \rangle_2 \\ &\approx \frac{1}{S^2} \sum_{i=1}^S \sum_{j=1}^S \langle \Phi(\mathbf{F}_{t,i}^m), \Phi(\mathbf{F}_{t+1,j}^m) \rangle, \end{aligned} \quad (1)$$

where $S = w \times h$ is the number of spatial locations, and $\langle \cdot, \cdot \rangle_2$ is the bilinear kernel. We approximate bilinear kernel via Tensor Sketch Projection Φ [10], aiming to reduce

the feature space dimension. The kernelized representation is then fed into a regression layer to predict the movement of b_t^m , leading to the corresponding proposal b_{t+1}^m in I_{t+1} . Accordingly, a set of proposals in the subsequent frames are obtained by estimating the movement of each proposal frame by frame, which are linked as the output tubelet.

3.2. Spatio-Temporal Complete Graph

With all the generated tubelets of each input video via TPN, we next present how to construct a spatio-temporal complete graph, that fully unfolds the inherent spatial and temporal interactions among all tubelets for reasoning. Specifically, we are given the set of L video clips and each video clip contains M tubelets, leading to the tubelet set $\mathcal{V} = \{v_i\}_{i=1}^{L \times M}$. By treating each tubelet as one graph node, we can build the spatio-temporal complete graph $\mathcal{G} = (\mathcal{V}, \mathcal{E})$, where \mathcal{E} denotes the set of densely connected graph edges between every two nodes. As depicted in Figure 2, we number all tubelets according to their spatio-temporal positions in the video: the spatially closer to the top left and the temporally earlier the tubelet, the smaller the number of that tubelet.

Graph Node. For each node $v \in \mathcal{V}$, we collect both visual & spatial information and represent it as the concatenation of tubelet visual feature \mathbf{f}_v^{visual} and the constituent bounding box coordinates \mathbf{f}_v^{coord} : $\mathbf{f}_v = [\mathbf{f}_v^{visual}, \mathbf{f}_v^{coord}]$.

To extract the visual feature of each tubelet in l -th clip, we first feed this clip (T consecutive frames) into a standard 3D CNN. The output of 3D CNN is a feature map with the size of $T \times W \times H \times D$ (T : temporal dimension; $H \times W$: spatial dimensions; D : channel number). Note that we do not utilize any temporal downsampling layers (either temporal pooling or time-strided convolutions) in 3D CNN, preserving the temporal fidelity as much as possible. Next, conditioned on the spatial coordinates of the bounding boxes across frames in tubelet, we perform RoI pooling over the output feature map of 3D CNN, followed by global max pooling to produce a D -dimensional visual representation \mathbf{f}_v^{visual} of that tubelet.

Considering that some actions are naturally rooted in the geometric properties (e.g., 2D location) of actors/objects, we further exploit the coordinates of constituent bounding boxes in the tubelet to represent each node. Specifically, the 2D location of the bounding box in each frame can be denoted as the 4-dimensional feature vector consisting of its center coordinates plus the height and width values. Thus, we represent the holistic location feature of each tubelet as a $4T$ -dimensional feature vector $\widehat{\mathbf{f}}_v^{coord}$, i.e., the concatenation of 2D locations across all frames. The holistic location feature of each tubelet is finally transformed into \mathbf{f}_v^{coord} via a Multi-Layer Perception (MLP).

Graph Edge. Most existing works (e.g., [48]) directly encapsulate the visual similarity and geometrical overlap

between two nodes into a scalar weight to represent each edge. This way apparently leaves the relative spatial relation or distance in between under-explored, and might result in failure of reasoning for distance-sensitive actions. Therefore, for each edge $e \in \mathcal{E}$, we derive a particular form of edge representation $\mathbf{f}_e = [\mathbf{f}_e^{sem}, \mathbf{f}_e^{coord}]$, which concatenates the semantic similarity \mathbf{f}_e^{sem} and relative coordinate changes \mathbf{f}_e^{coord} between nodes. The rational behind is to encourage the edge feature \mathbf{f}_e to reflect both semantic and relative spatial relations between tubelets, and thus facilitate the reasoning process.

Concretely, given two nodes v_i and v_j ($i < j$), we measure the semantic similarity between them as

$$f_{e_{ij}}^{sem} = \varphi(\mathbf{f}_{v_i}^{visual})^\top \varphi(\mathbf{f}_{v_j}^{visual}), \quad (2)$$

where $\mathbf{f}_{v_i}^{visual}$ and $\mathbf{f}_{v_j}^{visual}$ are the visual features of v_i and v_j , respectively. $\varphi(\cdot)$ denotes the feature transformation function. Moreover, depending on the holistic location features of v_i and v_j ($\widehat{\mathbf{f}}_{v_i}^{coord}, \widehat{\mathbf{f}}_{v_j}^{coord}$), we directly calculate the relative coordinate changes as $\widehat{\mathbf{f}}_{e_{ij}}^{coord} = \widehat{\mathbf{f}}_{v_i}^{coord} - \widehat{\mathbf{f}}_{v_j}^{coord}$. We further employ a MLP over $\widehat{\mathbf{f}}_{e_{ij}}^{coord}$ to obtain the final representation of relative coordinate changes $\mathbf{f}_{e_{ij}}^{coord}$.

3.3. Discriminative Sub-graphs

One natural way to perform spatio-temporal reasoning across actors/objects is to model the interactions between tubelets over the space-time complete graph. However, such complete graph might result in some irrelevant objects with regard to different action categories, and the overall stability of spatio-temporal reasoning will be inevitably affected. To alleviate this issue, our MUSLE learns to decompose the complete graph into a series of discriminative sub-graphs across different scales. The rational behind is to interpret each discriminative sub-graph as one prototype of each action category, that conveys greater discriminative power for the recognition of that action. Technically, we first extract multi-scale sub-graphs from the complete graph. Here each scale corresponds to a fixed number of nodes (i.e., 3, 4, or 5 nodes) in the sub-graphs. After that, for all sub-graphs from an identical action under each scale, we leverage a Gaussian Mixture Layer to interpret the distribution of them via Gaussian Mixture Model (GMM). K Gaussian kernels are thus achieved to represent the discriminative sub-graphs/action prototypes on that scale.

Gaussian Mixture Layer. Inspired by deep autoencoding Gaussian Mixture Model [8, 60], we utilize a Gaussian Mixture Layer to perform online clustering over all the sub-graphs to learn Gaussian kernels, rather than an offline training of GMM through standard EM algorithm [13]. Formally, given a set of N sub-graphs from an identical action on each scale, we represent each sub-graph as a feature vector \mathbf{x} by concatenating all the node and edge representations

within that sub-graph. Note that all nodes/edges are concatenated according to their assigned numbers (from small to large). Next, with the inputs of each sub-graph representation \mathbf{x} and an integer K (the number of mixture components/Gaussian kernels), we first leverage a MLP to predict the mixture membership of \mathbf{x} :

$$\boldsymbol{\alpha} = \text{MLP}(\mathbf{x}; \boldsymbol{\theta}), \quad \hat{\gamma} = \text{Softmax}(\boldsymbol{\alpha}), \quad (3)$$

where $\boldsymbol{\theta}$ is the network parameter and $\hat{\gamma}$ is a K -dimensional vector for the soft mixture membership prediction. After that, conditioned on all the mixture membership predictions of the N sub-graphs, the parameters of the k^{th} ($1 \leq k \leq K$) Gaussian kernel in GMM can be estimated as:

$$\begin{aligned} \hat{\phi}_k &= \sum_{n=1}^N \frac{\hat{\gamma}_{nk}}{N}, & \hat{\mu}_k &= \frac{\sum_{n=1}^N \hat{\gamma}_{nk} \mathbf{x}_n}{\sum_{n=1}^N \hat{\gamma}_{nk}} \\ \hat{\Sigma}_k &= \frac{\sum_{n=1}^N \hat{\gamma}_{nk} (\mathbf{x}_n - \hat{\mu}_k)(\mathbf{x}_n - \hat{\mu}_k)^\top}{\sum_{n=1}^N \hat{\gamma}_{nk}} \end{aligned} \quad (4)$$

where $\hat{\gamma}_n$ is the mixture membership prediction for the sub-graph \mathbf{x}_n . $\hat{\phi}_k$, $\hat{\mu}_k$, $\hat{\Sigma}_k$ denotes the mixture weight, mean, and covariance matrix for the k^{th} Gaussian kernel in GMM, respectively. Accordingly, with the estimated parameters of all Gaussian kernels, the possibility of sample \mathbf{x} belonging to the action category can be calculated as:

$$p(\mathbf{x}) = \sum_{k=1}^K \hat{\phi}_k \frac{\exp(-\frac{1}{2}(\mathbf{x} - \hat{\mu}_k)^\top \hat{\Sigma}_k^{-1} (\mathbf{x} - \hat{\mu}_k))}{\sqrt{|2\pi \hat{\Sigma}_k|}}, \quad (5)$$

where $|\cdot|$ denotes the determinant of a matrix.

Training Objective. At the training stage, we formulate the overall objective over all the N sub-graphs on each scale in a batch as:

$$\mathcal{L}(\boldsymbol{\theta}) = -\frac{1}{N} \sum_{n=1}^N \log p(\mathbf{x}_n) + \lambda R(\hat{\Sigma}), \quad (6)$$

where $p(\mathbf{x}_n)$ is the predicted possibility of each sub-graph \mathbf{x}_n calculated as in Eq. 5. $R(\hat{\Sigma}) = \sum_{k=1}^K \sum_{i=1}^{D_x} \frac{1}{\hat{\Sigma}_{kii}}$ (D_x : feature dimension of \mathbf{x}) is a regularization of covariance matrices $\hat{\Sigma}$, which restricts the diagonal entries in $\hat{\Sigma}$ converge to reasonable solution rather than 0. λ denotes the parameter for balancing the two parts, and we set it as 0.05 in practice. Since every operation within the Gaussian Mixture Layer is differentiable, we can easily propagate gradient from the Gaussian Mixture Layer to the tubelet feature extractor, and thus the two modules can be jointly optimized in an end-to-end manner.

Please note that instead of fixing the number of Gaussian kernels K under each scale for each action category, we employ a dynamic strategy to automatically update K along training process. Specifically, we initialize K with

a large value (6 in our case), and K will be decreased until all mixture weights of Gaussian kernels are higher than threshold th ($th = 0.02$) after one training epoch.

Inference. During inference, for each testing video, we first build the corresponding spatio-temporal complete graph, which is further decomposed into a group of sub-graphs across all the three scales. Next, for each action category, we utilize Eq. 5 to estimate the probability of each sub-graph belonging to that category conditioned on the learnt action prototypes. The highest probability across all sub-graphs under three scales is thus taken as the classification score of the testing video for this category. Finally, the action category with the highest classification score is regarded as the predicted category of the testing video.

4. Experiments

In this section, we empirically evaluate our MUSLE on two challenging action recognition benchmarks: Something-Something V1&V2 [11] and Kinetics-400 [2].

4.1. Datasets

Something-Something is one of the largest video datasets that focus on human-object interaction scenarios. The dataset contains 174 fine-grained categories of common human-object interactions with diverse objects and viewpoints. The recognition of them is challenging, which requires fine-grained understanding of the activity to distinguish similar actions within a group, e.g., “pushing something so that it falls off the table” and “pushing something so that it almost falls off but doesn’t.” The first version (V1) consists of around 108k videos in total, including 86k for training, 11k for validation, and 11k for testing. The second version (V2) further increases the video number to 220k. The average video length is 4.0 seconds and all videos are captured from object-centric view with fairly clean backgrounds. Thus, few scene contexts is required to be exploited for action recognition in this dataset, making it a natural choice of benchmark for evaluating spatio-temporal reasoning in videos (e.g., [22, 48]). Similarly, we mainly report the results of our MUSLE on this dataset to evaluate the capacity of spatio-temporal reasoning.

Kinetics-400 is a standard large-scale benchmark for action recognition, covering 400 action classes. It contains around 246k training videos and 20k validation videos. Each video in this dataset is 10-second short clip trimmed from the raw YouTube video. Here we additionally involve this dataset to further demonstrate the generalization of our proposal for action recognition.

4.2. Implementation Details

Training. At training stage, we adopt the same strategy as in TSN [47] to train our MUSLE framework. Specifically, given an input video, we first divide it into L ($L = 4$

Table 1. Performance contribution of each component in MUSLE. Experiments are conducted on Something-Something V2 validation set.

Method	Graph	Sub-graph	Node Coord	Edge Coord	Multi-scale	Top-1	Top-5
Base						60.8	86.5
Base+GCN [48]	✓					61.3	87.1
Base+GloRe [4]	✓					61.9	87.3
Base (3 nodes)	✓	✓				62.7	88.0
+Sub-graph (4 nodes)	✓	✓				63.2	88.3
(5 nodes)	✓	✓				62.2	87.5
+Node Coord (4 nodes)	✓	✓	✓			63.5	88.7
+Edge Coord (4 nodes)	✓	✓	✓	✓		64.1	89.3
MUSLE	✓	✓	✓	✓	✓	65.0	90.1

in our case) segments with equal durations, aiming to perform long-range temporal structure modeling. Then, for each segment, we randomly sample one clip consisting of 16 consecutive frames. The size of the short side of sampled frames is fixed to 256. We augment the data during training by scale and aspect-ratio jittering. For tubelet generation process, we utilize Faster R-CNN [34] pre-trained on COCO dataset [28] to detect objects in the first frame of each clip. Meanwhile, we pre-train the Tubelet Proposal Network [19] on ImageNet VID dataset [35] to estimate the movement of each object region frame by frame in each clip and fix its parameters during training. We select the top 8 tubelets with the highest detection scores in each clip to build the spatio-temporal complete graph, leading to 32 nodes in the complete graph for the whole video (consisting of 4 sampled clips). We capitalize on LGD network [33] as the tubelet feature extractor, which represents each tubelet as the outputs from the last convolutional layer with ROI Pooling. The parameters of the LGD network is initialized with the ImageNet pre-trained ResNet-50 model.

We implement MUSLE mainly on Caffe [14]. The whole framework is trained on four Tesla P40 GPUs via Stochastic Gradient Descent (SGD) with a mini-batch of 16 videos. The momentum and weight decay are set to 0.9 and 0.0005, respectively. We set the initial learning rate as 0.01, which is further divided by 10 after every 20 epochs. The training is stopped after 50 epoches.

Inference. During inference, we evenly sample 4 clips from each test video. For each frame in the clips, we follow the strategy in [15, 24] to resize the shorter size as 256 by maintaining the aspect ratio. We utilize the learnt Gaussian Mixture Model to compute the similarity between the sub-graphs extracted from the test video and action prototypes across all the scales and actions. The class of action prototype with the highest similarity is taken as the prediction.

4.3. Ablation Study of MUSLE

Here, we investigate how each design in MUSLE influences the overall performance. We start from a basic model (named **Base**) by feeding each video clip into LGD backbone and simply taking the output score as clip-level score. The averaged score over all clips is thus exploited for action classification. Base model solely capitalizes on the clip-

level holistic features, while leaving the object-level relations unexploited. As an alternative, **GCN** [48] leverages Tubelet Proposal Networks (TPN) to produce space-time actor/object tubelets for each clip. The representation of each tubelet is extracted through LGD backbone. After that, all the tubelets from clips within a video are taken as the graph nodes, which are connected with similarity relations in between. Graph Convolutional Network (GCN) is further utilized to perform spatio-temporal reasoning over the whole graph. The final video-level representation is thus obtained by performing mean pooling over all the refined graph nodes. **GloRe** [4] upgrades GCN with global reasoning unit, which conducts highly efficient global reasoning over the whole graph by projecting aggregated features over coordinate space into an interaction space. Instead of reasoning on the whole graph (e.g., GCN and GloRe), the run of **Base+Sub-graph** decomposes the whole graph (with only semantic similarity relations) into single-scale sub-graphs. For one specific scale, we utilize Gaussian Mixture Layer to learn the discriminative sub-graphs/action prototypes for action recognition. Please note that in Base+Sub-graph, we directly take the visual feature of LGD backbone to represent each tubelet. **Node Coord** further enhances tubelet representation by concatenating the visual feature and the coordinates of constituent proposals. In **Edge Coord**, the graph edges are strengthened to measure not only the semantic similarity between every two nodes, but also the relative coordinate changes in between. **Multi-scale** unifies the discriminative sub-graphs across all the three scales for action recognition.

Table 1 details the performances across different ways of reasoning about graph structure for action recognition on Something-Something V2. Specifically, for Base model, the use of original clip-level holistic features in general achieves a good performance. As expected, by additionally modeling the object-level relations over the whole spatio-temporal graph for recognizing actions, Base+GCN and Base+GloRe exhibit better performances than Base model. This generally verifies the merit of reasoning about spatio-temporal graph structure within videos. Nevertheless, performing reasoning over the whole graph would inevitably result in more irrelevant objects, which may affect the overall stability of reasoning process. To address this issue, our

Table 2. Comparison results of MUSLE with other state-of-the-art methods on Something-Something V1 & V2.

Method	Backbone	Pre-train	#Frames	Something-Something V1			Something-Something V2		
				top-1 val	top-5 val	top-1 test	top-1 val	top-5 val	top-1 test
TSN [47]	BNInception	ImageNet	16	19.7	46.6	-	27.8	57.6	-
TRN [58]	BNInception	ImageNet	8	34.4	-	33.6	48.8	77.6	50.9
DualAtt [49]	BNInception	ImageNet	8	-	-	-	51.6	80.3	54.0
TRG [56]	BNInception	ImageNet	16	45.9	74.9	-	56.7	79.9	-
I3D [2]	ResNet-50	Kinetics	32	41.6	72.2	-	-	-	-
I3D+GCN [48]	ResNet-50	Kinetics	32	43.3	75.1	-	-	-	-
NL I3D+GCN [48]	ResNet-50	Kinetics	32	46.1	76.8	45.0	-	-	-
S3D [50]	Inception	ImageNet	64	48.2	78.7	42.0	-	-	-
ECO [59]	BNInc+ResNet-18	Kinetics	16	41.4	-	-	-	-	-
TSM [27]	ResNet-50	Kinetics	16	47.2	77.1	46.0	63.4	88.5	64.3
STM [15]	ResNet-50	ImageNet	16	50.7	80.4	43.1	64.2	89.8	63.5
TEA [24]	ResNet-50	ImageNet	16	51.9	80.3	-	-	-	-
GSM [40]	InceptionV3	ImageNet	16	50.6	-	-	-	-	-
ASS [22]	ResNet-50	ImageNet	32	51.4	-	-	63.5	-	-
MUSLE	ResNet-50	ImageNet	16	52.5	81.6	47.4	65.0	90.1	65.0

unique design of Sub-graph enables the learning of single-scale discriminative sub-graphs as the prototypes of each action category for recognition. Here we vary the scale (i.e., node number) of sub-graphs in the range of $\{3, 4, 5\}$, and the results of Base+Sub-graph under different scales consistently outperform Base+GCN and Base+GloRe across all metrics. The best performances (Top-1: 63.2%, Top-5: 88.3%) are attained when the node number of each subgraph is set to 4. The results clearly highlight the advantage of exploiting sub-graphs in videos to represent and encode the discriminative patterns of each action. Furthermore, Node Coord and Edge Coord, which integrates Sub-graph with spatial-aware cues (i.e., information about proposal coordinates or relative coordinate changes), contributes an Top-1 accuracy increase of 0.3% and 0.6%, respectively. This demonstrates that Node Coord and Edge Coord are very practical choices to enhance the capacity of spatio-temporal reasoning, especially for the recognition of distance-sensitive actions (e.g., “moving something and something away from each other” versus “moving something and something closer to each other”). The integration of all sub-graphs across three scales, i.e., our MUSLE, reaches the highest performances for action recognition. The performance boosts basically indicate the advantage of multi-scale aggregation of sub-graphs during reasoning, that enables flexibility in the scale of sub-graphs to better reflect the inherent properties of various actions.

4.4. Comparisons with State-of-the-Arts

Something-Something. Table 2 summarizes the quantitative results of our MUSLE on both Something-Something V1 and V2 datasets. We compare MUSLE with several existing state-of-the-art action recognition methods, which can be grouped into two directions: 2D CNNs based techniques (e.g., TSN, TRN, and TRG) and 3D/(2+1)D CNNs based approaches (e.g., I3D, I3D+GCN, S3D, and ASS). Overall, the results under the same backbone (ResNet-50) across different datasets consistently demonstrate that our

MUSLE exhibits better performances than other 2D and 3D/(2+1)D CNNs based models. In particular, the Top-1 val accuracy of MUSLE can achieve 52.5% and 65.0% on Something-Something V1 and V2 respectively, which makes 0.6% and 0.8% absolute improvements over the best competitors TEA and STM. By modeling temporal orders across frames for reasoning, TRN achieves better performances than TSN which simply averages the features of temporal frames. Moreover, DualAtt improves TRN by additionally capturing human-object interactions via attention mechanism. TRG further leads to a performance boost by constructing a temporal relation graph to capture the long-range temporal dependencies across frames. For 3D/(2+1)D CNNs based approaches, I3D+GCN by exploiting the relations between objects for spatio-temporal reasoning over the whole graph, outperforms I3D. Different from the manually-designed graph-based reasoning module in I3D+GCN and NL I3D+GCN, ASS automatically searches adaptive interaction modeling structures for reasoning on space-time graph, and achieves better performance. Nevertheless, the performances of ASS are still lower than our MUSLE, which uniquely discovers the discriminative sub-graphs for action recognition. This confirms the advantage of decomposing the whole graph into sub-graphs and modeling the discriminative ones for spatio-temporal reasoning in MUSLE.

Figure 3 showcases the most similar sub-graphs w.r.t the learnt action prototypes in three test videos. We also display some intuitive interpretations of semantic and relative spatial relations behind the graph edges. From these exemplar results, it is easy to see that our learnt discriminative sub-graphs/action prototypes via MUSLE can capture the discriminative patterns of actions and thus facilitate action recognition. For instance, by encoding the patterns of “two key objects are getting closer” into the sub-graph of the second video, it is nature to recognize the action of “Moving something closer to something”.

Kinetics-400. To further verify the generality of our pro-

Table 3. Comparison results of MUSLE with other state-of-the-art methods on Kinetics-400 validation set.

Method	Backbone	Top-1	Top-5
TSN [47]	BNInception	69.1	88.7
I3D [2]	InceptionV1	71.1	89.3
R(2+1)D [43]	ResNet-34	72.0	90.0
LGD [33]	ResNet-50	73.1	91.2
ECO [59]	BNInc+ResNet-18	70.7	89.4
TSM [27]	ResNet-50	72.5	90.7
STM [15]	ResNet-50	73.7	91.6
TEA [24]	ResNet-50	74.0	91.3
MUSLE	ResNet-50	75.1	92.0

Table 4. Performance comparison on UCF101 and HMDB51.

Method	Pre-train	Finetune	UCF101	HMDB51
LGD [33]	Kinetics	No	80.5	52.3
LGD [33]	Kinetics	Yes	93.2	70.1
MUSLE	Kinetics	No	90.1	65.8
MUSLE	Kinetics	Yes	94.8	72.2

posed MUSLE, we additionally conduct experiments for action recognition in the standard benchmark of Kinetics-400. Note that different from Something-Something which consists of object-centric videos with clean backgrounds, Kinetics-400 includes plenty of human-centric videos with complex backgrounds and some action categories (e.g., “laughing” and “jogging”) are related to few objects. This naturally makes the reasoning over objects in Kinetics-400 more challenging than Something-Something. However, as shown in Table 3, our MUSLE still manages to achieve competitive results against state-of-the-art techniques without graph-based reasoning. The results again verify the idea of exploiting multi-scale sub-graphs to reason about the dynamics of object interactions for action recognition.

4.5. Cross-Dataset Validation

Recall that our MUSLE learns to discover prototypical sub-graphs/action prototypes that reflect the discriminative patterns for each human action. Such learnt action prototypes are generic, and could potentially be dataset-invariant, i.e., benefiting the recognition of actions in a target dataset different from the source training dataset. To evaluate this idea, we perform cross-dataset validation by pre-learning action prototypes on Kinetics-400 dataset and further leveraging them to classify videos in UCF101 [39] and HMDB51 [17] datasets without or with fine-tuning. Here we select 44 and 16 action categories in UCF101 and HMDB51 respectively for evaluation, which also appear in the source training dataset (Kinetics-400). Details of the selected action categories in each target dataset can be referred in supplementary material. As shown in Table 4, under the most challenging setting without any fine-tuning, the accuracy of our MUSLE can achieve 90.1% and 65.8% on UCF101 and HMDB51, making 9.6% and 13.5% absolute improvements over LGD. Moreover, when further fine-tuning on target

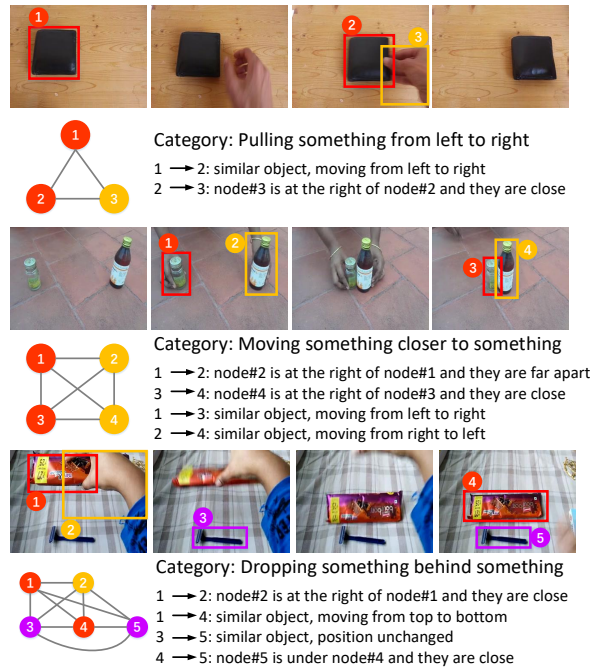


Figure 3. Examples showing the most similar sub-graphs with regard to the learnt action prototypes for three test videos. We only show the middle frame for each sampled video clip. Each sub-graph is equipped with several intuitive interpretations of semantic and relative spatial relations behind the graph edges.

datasets, our MUSLE still outperforms LGD. The results generally confirm the transferability of learnt action prototypes across different datasets in our MUSLE.

5. Conclusion

We have proposed Multi-scale Sub-graph LEarning (MUSLE) framework, which explores the discriminative patterns of each action for recognition in videos. Particularly, we study the problem from the viewpoint of presenting the video structure as a space-time graph, decomposing such graph into sub-graphs, and interpreting the discriminative ones as action prototypes. To materialize our idea, we first link the region proposals across frames as tubelets, and build the spatio-temporal graph with nodes of tubelets and edges of dense connectivity. The graph is decomposed into multi-scale sub-graphs to characterize the complexity of different actions. Then, MUSLE learns a Gaussian Mixture Layer to estimate the distribution of sub-graphs from one certain action on each scale and takes Gaussian kernels as the prototypical structures of such action for recognition. Experiments conducted on three datasets, i.e., Something-Something V1 & V2, and Kinetics-400, validate our proposal and analysis. More remarkably, our MUSLE achieves the superior accuracy on Something-Something V2.

Acknowledgments. This work was supported by the National Key R&D Program of China under Grant No. 2020AAA0108600.

References

- [1] Gedas Bertasius, Lorenzo Torresani, Stella X Yu, and Jianbo Shi. Convolutional random walk networks for semantic image segmentation. In *CVPR*, 2017. 2
- [2] Joao Carreira and Andrew Zisserman. Quo vadis, action recognition? a new model and the kinetics dataset. In *CVPR*, 2017. 2, 5, 7, 8
- [3] Siddhartha Chandra, Nicolas Usunier, and Iasonas Kokkinos. Dense and low-rank gaussian crfs using deep embeddings. In *ICCV*, 2017. 2
- [4] Yunpeng Chen, Marcus Rohrbach, Zhicheng Yan, Yan Shuicheng, Jiashi Feng, and Yannis Kalantidis. Graph-based global reasoning networks. In *CVPR*, 2019. 2, 6
- [5] Zhiwei Deng, Arash Vahdat, Hexiang Hu, and Greg Mori. Structure inference machines: Recurrent neural networks for analyzing relations in group activity recognition. In *CVPR*, 2016. 2
- [6] Ali Diba, Vivek Sharma, and Luc Van Gool. Deep temporal linear encoding networks. In *CVPR*, 2017. 2
- [7] Quanfu Fan, Chun-Fu Richard Chen, Hilde Kuehne, Marco Pistoia, and David Cox. More is less: Learning efficient video representations by big-little network and depthwise temporal aggregation. In *NIPS*, 2019. 2
- [8] Yaxiang Fan, Gongjian Wen, Deren Li, Shaohua Qiu, Martin D Levine, and Fei Xiao. Video anomaly detection and localization via gaussian mixture fully convolutional variational autoencoder. *Computer Vision and Image Understanding*, 2020. 4
- [9] Christoph Feichtenhofer, Axel Pinz, and Andrew Zisserman. Convolutional two-stream network fusion for video action recognition. In *CVPR*, 2016. 2
- [10] Yang Gao, Oscar Beijbom, Ning Zhang, and Trevor Darrell. Compact bilinear pooling. In *CVPR*, 2016. 3
- [11] Raghav Goyal, Samira Ebrahimi Kahou, Vincent Michalski, Joanna Materzynska, Susanne Westphal, Heuna Kim, Valentin Haenel, Ingo Fruend, Peter Yianilos, Moritz Mueller-Freitag, et al. The “something something” video database for learning and evaluating visual common sense. In *ICCV*, 2017. 5
- [12] Kaiming He, Xiangyu Zhang, Shaoqing Ren, and Jian Sun. Deep residual learning for image recognition. In *CVPR*, 2016. 2
- [13] Peter J Huber. *Robust statistics*, volume 523. John Wiley & Sons, 2004. 4
- [14] Yangqing Jia, Evan Shelhamer, Jeff Donahue, Sergey Karayev, Jonathan Long, Ross Girshick, Sergio Guadarrama, and Trevor Darrell. Caffe: Convolutional architecture for fast feature embedding. In *ACM MM*, 2014. 6
- [15] Boyuan Jiang, MengMeng Wang, Weihao Gan, Wei Wu, and Junjie Yan. Strm: Spatiotemporal and motion encoding for action recognition. In *ICCV*, 2019. 6, 7, 8
- [16] Thomas N Kipf and Max Welling. Semi-supervised classification with graph convolutional networks. In *ICLR*, 2017. 2
- [17] Hildegarde Kuehne, Hueihan Jhuang, Estibaliz Garrote, Tomaso Poggio, and Thomas Serre. Hmdb: a large video database for human motion recognition. In *ICCV*, 2011. 8
- [18] Heeseung Kwon, Manjin Kim, Suha Kwak, and Minsu Cho. Motionsqueeze: Neural motion feature learning for video understanding. 2020. 2
- [19] Dong Li, Zhaofan Qiu, Qi Dai, Ting Yao, and Tao Mei. Recurrent tubelet proposal and recognition networks for action detection. In *ECCV*, 2018. 3, 6
- [20] Dong Li, Ting Yao, Ling-Yu Duan, Tao Mei, and Yong Rui. Unified spatio-temporal attention networks for action recognition in videos. *IEEE Transactions on Multimedia*, 2018. 2
- [21] Dong Li, Ting Yao, Zhaofan Qiu, Houqiang Li, and Tao Mei. Long short-term relation networks for video action detection. In *ACM MM*, 2019. 2
- [22] Haoxin Li, Wei-Shi Zheng, Yu Tao, Haifeng Hu, and Jian-Huang Lai. Adaptive interaction modeling via graph operations search. In *CVPR*, 2020. 2, 5, 7
- [23] Yin Li and Abhinav Gupta. Beyond grids: Learning graph representations for visual recognition. In *NIPS*, 2018. 2
- [24] Yan Li, Bin Ji, Xintian Shi, Jianguo Zhang, Bin Kang, and Limin Wang. Tea: Temporal excitation and aggregation for action recognition. In *CVPR*, 2020. 6, 7, 8
- [25] Yujia Li, Daniel Tarlow, Marc Brockschmidt, and Richard Zemel. Gated graph sequence neural networks. In *ICLR*, 2016. 2
- [26] Xiaodan Liang, Zhiting Hu, Hao Zhang, Liang Lin, and Eric P Xing. Symbolic graph reasoning meets convolutions. In *NIPS*, 2018. 2
- [27] Ji Lin, Chuang Gan, and Song Han. Tsm: Temporal shift module for efficient video understanding. In *ICCV*, 2019. 2, 7, 8
- [28] Tsung-Yi Lin, Michael Maire, Serge Belongie, James Hays, Pietro Perona, Deva Ramanan, Piotr Dollár, and C Lawrence Zitnick. Microsoft coco: Common objects in context. In *ECCV*, 2014. 3, 6
- [29] Fuchen Long, Ting Yao, Zhaofan Qiu, Xinmei Tian, Jiebo Luo, and Tao Mei. Gaussian temporal awareness networks for action localization. In *CVPR*, 2019. 2
- [30] Fuchen Long, Ting Yao, Zhaofan Qiu, Xinmei Tian, Jiebo Luo, and Tao Mei. Learning to localize actions from moments. In *ECCV*, 2020. 2
- [31] Zhaofan Qiu, Ting Yao, and Tao Mei. Deep quantization: Encoding convolutional activations with deep generative model. In *CVPR*, 2017. 2
- [32] Zhaofan Qiu, Ting Yao, and Tao Mei. Learning spatio-temporal representation with pseudo-3d residual networks. In *ICCV*, 2017. 2
- [33] Zhaofan Qiu, Ting Yao, Chong-Wah Ngo, Xinmei Tian, and Tao Mei. Learning spatio-temporal representation with local and global diffusion. In *CVPR*, 2019. 2, 6, 8
- [34] Shaoqing Ren, Kaiming He, Ross Girshick, and Jian Sun. Faster r-cnn: Towards real-time object detection with region proposal networks. In *NIPS*, 2015. 6
- [35] Olga Russakovsky, Jia Deng, Hao Su, Jonathan Krause, Sanjeev Satheesh, Sean Ma, Zhiheng Huang, Andrej Karpathy, Aditya Khosla, Michael Bernstein, et al. Imagenet large scale visual recognition challenge. *International journal of computer vision*, 2015. 2, 6

- [36] Franco Scarselli, Marco Gori, Ah Chung Tsoi, Markus Hagenbuchner, and Gabriele Monfardini. The graph neural network model. *IEEE Transactions on Neural Networks*, 2008. 2
- [37] Karen Simonyan and Andrew Zisserman. Two-stream convolutional networks for action recognition in videos. In *NIPS*, 2014. 2
- [38] Karen Simonyan and Andrew Zisserman. Very deep convolutional networks for large-scale image recognition. In *ICLR*, 2015. 2
- [39] Khurram Soomro, Amir Roshan Zamir, and Mubarak Shah. Ucf101: A dataset of 101 human actions classes from videos in the wild. *arXiv preprint arXiv:1212.0402*, 2012. 8
- [40] Swathikiran Sudhakaran, Sergio Escalera, and Oswald Lanz. Gate-shift networks for video action recognition. In *CVPR*, 2020. 7
- [41] Christian Szegedy, Wei Liu, Yangqing Jia, Pierre Sermanet, Scott Reed, Dragomir Anguelov, Dumitru Erhan, Vincent Vanhoucke, and Andrew Rabinovich. Going deeper with convolutions. In *CVPR*, 2015. 2
- [42] Du Tran, Lubomir Bourdev, Rob Fergus, Lorenzo Torresani, and Manohar Paluri. Learning spatiotemporal features with 3d convolutional networks. In *ICCV*, 2015. 2
- [43] Du Tran, Heng Wang, Lorenzo Torresani, Jamie Ray, Yann LeCun, and Manohar Paluri. A closer look at spatiotemporal convolutions for action recognition. In *CVPR*, 2018. 2, 8
- [44] Chuanming Wang, Huiyuan Fu, Charles X Ling, Peilun Du, and Huadong Ma. Region-based global reasoning networks. In *AAAI*, 2020. 2
- [45] Heng Wang, Alexander Kläser, Cordelia Schmid, and Cheng-Lin Liu. Action recognition by dense trajectories. In *CVPR*, 2011. 2
- [46] Heng Wang and Cordelia Schmid. Action recognition with improved trajectories. In *ICCV*, 2013. 2
- [47] Limin Wang, Yuanjun Xiong, Zhe Wang, Yu Qiao, Dahua Lin, Xiaoou Tang, and Luc Van Gool. Temporal segment networks: Towards good practices for deep action recognition. In *ECCV*, 2016. 2, 5, 7, 8
- [48] Xiaolong Wang and Abhinav Gupta. Videos as space-time region graphs. In *ECCV*, 2018. 2, 4, 5, 6, 7
- [49] Tete Xiao, Quanfu Fan, Dan Gutfreund, Mathew Monfort, Aude Oliva, and Bolei Zhou. Reasoning about human-object interactions through dual attention networks. In *ICCV*, 2019. 7
- [50] Saining Xie, Chen Sun, Jonathan Huang, Zhuowen Tu, and Kevin Murphy. Rethinking spatiotemporal feature learning: Speed-accuracy trade-offs in video classification. In *ECCV*, 2018. 2, 7
- [51] Sijie Yan, Yuanjun Xiong, and Dahua Lin. Spatial temporal graph convolutional networks for skeleton-based action recognition. In *AAAI*, 2018. 2
- [52] Xu Yang, Kaihua Tang, Hanwang Zhang, and Jianfei Cai. Auto-encoding scene graphs for image captioning. In *CVPR*, 2019. 2
- [53] Ting Yao, Yingwei Pan, Yehao Li, and Tao Mei. Exploring visual relationship for image captioning. In *ECCV*, 2018. 2
- [54] Ting Yao, Yiheng Zhang, Zhaofan Qiu, Yingwei Pan, and Tao Mei. Seco: Exploring sequence supervision for unsupervised representation learning. In *AAAI*, 2021. 2
- [55] Joe Yue-Hei Ng, Matthew Hausknecht, Sudheendra Vijayanarasimhan, Oriol Vinyals, Rajat Monga, and George Toderici. Beyond short snippets: Deep networks for video classification. In *CVPR*, 2015. 2
- [56] Jingran Zhang, Fumin Shen, Xing Xu, and Heng Tao Shen. Temporal reasoning graph for activity recognition. *IEEE Transactions on Image Processing*, 2020. 7
- [57] Yiwu Zhong, Liwei Wang, Jianshu Chen, Dong Yu, and Yin Li. Comprehensive image captioning via scene graph decomposition. In *ECCV*, 2020. 2
- [58] Bolei Zhou, Alex Andonian, Aude Oliva, and Antonio Torralba. Temporal relational reasoning in videos. In *ECCV*, 2018. 7
- [59] Mohammadreza Zolfaghari, Kamaljeet Singh, and Thomas Brox. Eco: Efficient convolutional network for online video understanding. In *ECCV*, 2018. 2, 7, 8
- [60] Bo Zong, Qi Song, Martin Renqiang Min, Wei Cheng, Cristian Lumezanu, Daeki Cho, and Haifeng Chen. Deep autoencoding gaussian mixture model for unsupervised anomaly detection. In *ICLR*, 2018. 4